

FEMS Microbiology Letters, Vol. 151 (1) (1997) pp. 65-70

Copyright (c) 1997 Federation of European Microbiological Societies. Published by Elsevier Science B.V.

PII: S0378-1097(97)00139-0

M protein mediated adhesion of M type 24 *Streptococcus pyogenes* stimulates release of interleukin-6 by HEp-2 tissue culture cells

Harry S. Courtney^{a,b}, Itzhak Ofek^c and David L. Hasty^{a,d}

^a Veterans Affairs Medical Center, University of Tennessee, Memphis, TN, USA

^b Department of Medicine, University of Tennessee, Memphis, TN, USA

^d Department of Anatomy and Neurobiology, University of Tennessee, Memphis, TN, USA

^c Department of Human Microbiology, Sackler Faculty of Medicine, Tel-Aviv University, Tel-Aviv, Israel

Received 6 February 1997; revised 25 March 1997; accepted 26 March 1997

Abstract


We investigated the contributions of lipoteichoic acid and M protein to reversible and irreversible adhesion of group A streptococci and the effects of such adhesion on release of interleukin-6. Streptococci in which lipoteichoic acid was masked by the hyaluronate capsule were readily washed from HEp-2 cells, indicating no attachment. Unencapsulated, M-negative streptococci in which lipoteichoic acid was exposed were removed more slowly, indicating loose attachment. Only unencapsulated streptococci that expressed both lipoteichoic acid and M protein remained stably adherent to HEp-2 cells throughout multiple washes. Streptococci expressing both M protein and lipoteichoic acid induced release of interleukin-6 from HEp-2 cells, whereas an isogenic, M-negative mutant failed to induce release of interleukin-6. These data suggest that lipoteichoic acid mediates reversible adhesion and that M protein is required for irreversible adhesion and for inducing release of interleukin-6 from HEp-2 cells.

Keyword(s): *Streptococcus pyogenes*; M protein; Cytokine

Copyright ©1996-2002 Federation of European Microbiological Societies. All rights reserved.

Note: Our access control system is due to be updated shortly. You will then need to register and select a username and password to access full text, even if you have not had to do so in the past.

[Click here for more information.](#)

PDF files should be viewed and printed using Adobe® Acrobat® Reader version 3.01 or higher.  [More information](#) about PDF and Adobe® Acrobat® Reader.

Antimicrobial Agents and Chemotherapy, September 2000, p. 2578-2580, Vol. 44, No. 9

0066-4804/00/\$04.00+0

Copyright © 2000, American Society for Microbiology. All rights reserved.

Inhibitory Effects of Plant Polyphenoloxidase on Colonization Factors of *Streptococcus sobrinus* 6715

M. M. Cowan,^{1,*} E. A. Horst,¹ S. Luengpailin,² and R. J. Doyle²

Department of Microbiology, Miami University, Oxford, Ohio 45056,¹ and Department of Microbiology and Immunology, Health Sciences Center, University of Louisville, Louisville, Kentucky 40292²

Received 10 January 2000/Returned for modification 13 April 2000/Accepted 13 June 2000

► ABSTRACT

Exogenously added polyphenoloxidase (EC 1.14.18.1), an enzyme which oxidizes tyrosine residues and is commonly found in many dietary components, abolished the aggregation of *Streptococcus sobrinus* 6715 by high-molecular-weight dextran. The enzyme decreased glucan-binding lectin and/or glucosyltransferase I activities.

▲ [Top](#)
• [Abstract](#)
▼ [Text](#)
▼ [References](#)

► TEXT

In the past three decades, rapid progress has been made in the understanding of microbial adhesion (8). A wealth of research has established that *Streptococcus sobrinus* must attach to glucans deposited on the tooth surface for successful colonization of the oral cavity (4, 6, 17). For this purpose it uses a glucan-binding lectin (GBL) and a family of glucosyltransferases (GTFs). GTFs are composed of a C-terminal glucan-binding domain supplemented by an N-terminal catalytic peptide (7). Both GBL and GTFs have been shown to possess critical tyrosines in their glucan-binding sites (15). In this study we investigated the effect on adhesion of bacterial pretreatment with polyphenoloxidase (PPO) (EC 1.14.18.1). PPO is an enzyme found in many plant species, including most noncitrus European fruits and many vegetables (18). It possesses two activities, oxidizing a variety of phenolic substrates, including tyrosine, to L-dihydroxyphenylalanine and then to quinones. This action results in browning when it occurs in fruits, such as apples and bananas. Plants and invertebrates may use the PPO system, with its resultant tannin production, as a defense against invasion by predators, such as fungi and insects (11,

▲ [Top](#)
▲ [Abstract](#)
• [Text](#)
▼ [References](#)

12).

S. sobrinus 6715 was maintained and grown either on tryptic soy agar or in the defined medium of Terleckyj et al. (16). The standard rate assay of Drake et al. (3) was used to study the interaction of *S. sobrinus* 6715 GBL with high-molecular-weight dextran. Briefly, bacterial suspensions were mixed with dextran T-2000 (10 μ g/ml), and the decrease in optical density was continuously monitored spectrophotometrically for 5 min. Absorption at 540 nm was used to calculate $\ln(A/A_0)$ (A , observed optical density; A_0 , optical density at time zero), which was plotted versus time in minutes. Each sample was assayed in triplicate. For enzyme treatments, cells were incubated with PPO (from mushrooms; Worthington Biochemical Corporation, Freehold, N.J.) (180 to 1,260 U/ml) for 1 h at 37°C.

Figure 1 depicts the decrease in absorption for control and PPO-treated (464 U/ml) *S. sobrinus* 6715 after mixing with glucan (T-2000). Bacteria in this experiment were grown in complex medium. Cells grown in defined medium required sevenfold-lower concentrations of PPO for inhibition (data not shown). PPO pretreatment reduced aggregate formation to approximately the level seen when a competitive binding inhibitor, low-molecular-weight glucan (dextran T-10), was included in the reaction (Fig. 1). When dextran T-10 was added to cells before enzyme treatment, the action of PPO was blocked. Addition of glycogen prior to PPO treatment had no effect on PPO's activity.

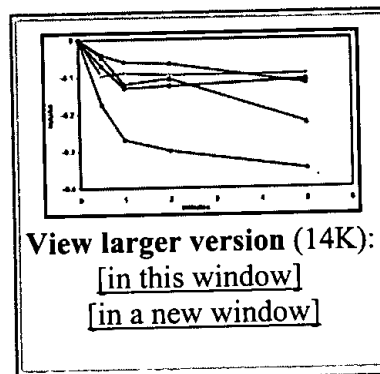


FIG. 1. Inhibition of aggregation of *S. sobrinus* by high-molecular-weight dextran after treatment with PPO. High-molecular-weight dextran (dextran T-2000) was added as a last step in all tubes. ♦, control (*S. sobrinus*); ×, low-molecular-weight dextran (T-10) plus *S. sobrinus*; ●, *S. sobrinus* pretreated with PPO; ▲, dextran T-10 added to *S. sobrinus* before PPO treatment; ■, glycogen added to *S. sobrinus* before PPO treatment. Experiments were performed in triplicate.

The following known PPO inhibitors prevented the enzyme from abolishing aggregation of *S. sobrinus* by glucan: EDTA (5 mM), 100% decrease in PPO activity; potassium chloride (200 mM), 100% decrease; polyvinylpyrrolidone (500 μ g/ml), 100% decrease; ascorbic acid (3 mM), 100% decrease; and lactic acid (10% [wt/vol]), 91% decrease. Protease inhibitors, phenylmethylsulfonyl fluoride (500 μ M) and leupeptin (500 μ g/ml), were also tested to ensure that the activity was not due to possible contaminating proteases in the enzyme batches. Neither decreased the action of PPO. Incubation of inhibitors with *S. sobrinus* had no effect on control glucan-dependent aggregation. All inhibitors were from Sigma.

PPO was mixed (by gentle vortexing) with *S. sobrinus*-glucan complexes after 30 min of control aggregation (Fig. 2). Reformation of aggregates was significantly retarded with respect to the control bacteria. After another 30 min the complexes were vortexed again (to disrupt aggregates) with no further addition of PPO. PPO-containing tubes continued to show slower and less complete aggregation, suggesting either that PPO enzymatically altered the binding site or that it bound with a higher affinity than dextran.

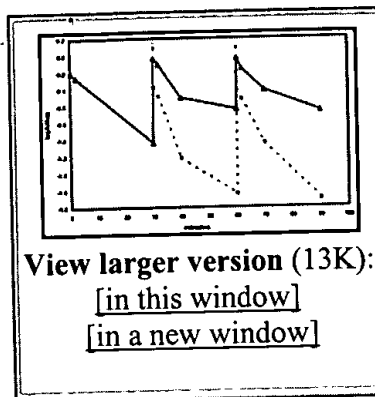


FIG. 2. Prevention of reaggregation of *S. sobrinus* by addition of PPO. ■, control, *S. sobrinus* plus glucan T-2000; ▲, *S. sobrinus* plus glucan T-2000 plus PPO. Arrow 1 shows when PPO was added with vortexing, and arrow 2 shows when the complexes were vortexed with no further addition of PPO. Experiments were performed in triplicate.

Growth vessel pellicle formation, mediated by the combined activity of GTFs and GBL (17), was investigated. Bacteria were inoculated into 5-ml tubes of tryptic soy broth with and without sucrose (200 mM) and/or PPO (1.0 mg/ml). After 18 h of growth, tubes were emptied, stained with crystal violet, and visually examined. Only PPO-containing cultures produced no pellicles in the presence of sucrose (data not shown).

The ability of PPO to reduce the activity of partially purified GTFs was assayed as follows. PPO-treated (50 U/ml) and untreated crude GTFs obtained through ammonium sulfate precipitation of *S. sobrinus* culture supernatant were subjected to nondenaturing electrophoresis in polyacrylamide. The presence of glucan-binding bands was demonstrated by incubating duplicate gels in fluorescein isothiocyanate-conjugated glucan T-10 (2 mg/ml). GTF activity was assayed by incubating gels in sucrose followed by development with Schiff's reagent. Of four discrete bands which bound glucan, two (molecular weight, 145,000 and 135,000) demonstrated GTF activity. The higher-molecular-weight band, corresponding to the reported size (15) of GTF-I (an isoenzyme producing insoluble glucan), lost activity after incubation with PPO. Glucan-binding activity has been shown to reside both on glucan-binding proteins (with no catalytic activity) and on the C-terminal end of GTFs (5, 7, 15). Further study is needed to determine which of the family of glucan-binding proteins is affected by PPO. A combination of GBL and GTF-I inhibition could have a potentially powerful effect on oral ecology.

Disk diffusion (100 U of PPO) and broth dilution assays (in tryptic soy broth) of PPO (highest PPO concentration = 464 U/ml) showed that PPO did not prevent growth of *S. sobrinus* (data not shown).

PPO is a copper-requiring metalloenzyme. Therefore, metal-chelating agents have been found to be inhibitory to its activity (19). The PPO inhibition by EDTA, ascorbic acid, and lactic acid seen in this study supports this finding and suggests that naturally occurring chelators, such as lactic acid manufactured by oral streptococci, could have similar effects in vivo and could conceivably be an adaptive response by the bacteria to the constant presence of dietary PPO originating in fruits and vegetables. Various studies report that persons consuming large quantities of fruits and vegetables do indeed have lower caries rates (10). It is plausible, based on the present results, that PPO may play some role as an anticaries agent.

There are many examples of the importance of tyrosine in carbohydrate-binding sites of microbial proteins (1, 2, 9, 13, 14, 20, 21). If tyrosine is indeed a "consensus" residue necessary for the specific binding of multiple microbial pathogens to host tissues, alteration of tyrosine could represent a broad-spectrum approach to the prevention and interruption of microbial attachment and biofilm formation.

▶ ACKNOWLEDGMENTS

This project was supported by funding from Genencor International and NIDCR to R.J.D. and M.M.C. and by the Miami University Office for the Advancement of Science and Teaching (M.M.C.).

▶ FOOTNOTES

* Corresponding author. Mailing address: Department of Microbiology, Miami University, Oxford, OH 45056. Phone: (513) 727-3231. Fax: (513) 727-3367. E-mail: cowanmm@muohio.edu.

▶ REFERENCES

▲ [Top](#)
 ▲ [Abstract](#)
 ▲ [Text](#)
 • [References](#)

1. **Cornelissen, C. N., J. E. Anderson, and P. F. Sparling.** 1997. Characterization of the diversity and the transferrin-binding domain of gonococcal transferrin-binding protein 2. *Infect. Immun.* **65**:822-828[[Abstract](#)].
2. **Doyle, R. J., and O. A. Roholt.** 1967. Tyrosyl involvement in the concanavalin A-polysaccharide precipitin reaction. *Life Sci.* **7**:841-846.
3. **Drake, D., K. G. Taylor, A. S. Bleiweis, and R. J. Doyle.** 1988. Specificity of the glucan-binding lectin of *Streptococcus cricetus*. *Infect. Immun.* **56**:1864-1872[[Medline](#)].
4. **Gibbons, R. J., and R. J. Fitzgerald.** 1969. Dextran-induced agglutination of *Streptococcus mutans*, and its potential role in the formation of microbial dental plaques. *J. Bacteriol.* **98**:341-346[[Medline](#)].
5. **Jespersgaard, C., G. Hajishengallis, T. E. Greenway, D. J. Smith, M. W. Russell, and S. M. Michalek.** 1999. Functional and immunogenic characterization of two cloned regions of *Streptococcus mutans* glucosyltransferase I. *Infect. Immun.* **67**:810-816[[Abstract/Full Text](#)].
6. **Koga, T., H. Asakawa, N. Okahashi, and S. Hamada.** 1986. Sucrose-dependent cell adherence and cariogenicity of serotype c *Streptococcus mutans*. *J. Gen. Microbiol.* **132**:2873-2883[[Medline](#)].
7. **Mooser, G., and C. Wong.** 1988. Isolation of a glucan-binding domain of glucosyltransferase (1,6- α -glucan synthase) from *Streptococcus sobrinus*. *Infect. Immun.* **56**:880-884[[Medline](#)].
8. **Ofek, I., and R. J. Doyle.** 1994. Bacterial adhesion to cells and tissues. Chapman and Hall, New York, N.Y.
9. **Quioco, F. A.** 1986. Carbohydrate-binding proteins: tertiary structures and protein-sugar interactions. *Annu. Rev. Biochem.* **55**:287-315[[Medline](#)].
10. **Rahmatulla, M., and E. E. Guile.** 1990. Relationship between dental caries and vegetarian and non-vegetarian diets. *Community Dent. Oral Epidemiol.* **18**:277-278[[Medline](#)].
11. **Ratcliffe, N. A.** 1985. Invertebrate immunity for the non-specialist. *Immunol. Lett.* **10**:253-270[[Medline](#)].
12. **Scalbert, A.** 1991. Antimicrobial properties of tannins. *Phytochemistry* **30**:3875-3883[[CrossRef](#)].
13. **Schembri, M. A., L. Pallesen, H. Connell, D. L. Hasty, and P. Klemm.** 1996. Linker insertion analysis of the FimH adhesin of type 1 fimbriae in an *Escherichia coli* FimH null background. *FEBS*

- analysis of the fimbrii adhesin of type 1 fimbriae in an *Escherichia coli* fimbrii-null background. *FEMS Microbiol. Lett.* **137**:257-263[CrossRef][Medline].
14. Singh, J. S., K. G. Taylor, and R. J. Doyle. 1993. Essential amino acids involved in glucan-dependent aggregation of *Streptococcus sobrinus*. *Carbohydr. Res.* **244**:137-147[Medline].
 15. Smith, D. J., W. F. King, C. D. Wu, B. I. Shen, and M. A. Taubman. 1998. Structural and antigenic characteristics of *Streptococcus sobrinus* glucan binding proteins. *Infect. Immun.* **66**:5565-5569[Abstract/Full Text].
 16. Terleckyj, B., N. P. Willett, and G. D. Shockman. 1975. Growth of several cariogenic strains of oral streptococci in a chemically defined medium. *Infect. Immun.* **11**:649-655[Medline].
 17. Vacca-Smith, A. M., A. R. Venkitaraman, R. G. Quivey, Jr., and W. H. Bowen. 1996. Interactions of streptococcal glucosyltransferases with α -amylase and starch on the surface of saliva-coated hydroxyapatite. *Arch. Oral Biol.* **41**:291-298[Medline].
 18. Vámos-Vigyazo, L. 1981. Polyphenol oxidase and peroxidase in fruits and vegetables. *Crit. Rev. Food Sci. Nutr.* **15**:49-127[Medline].
 19. Walker, J. R. L. 1975. Enzymic browning in food. *Enzyme Technol. Dig.* **4**:89.
 20. Weis, W., J. H. Brown, S. Cusak, J. C. Paulson, J. J. Skehel, and D. C. Wiley. 1988. Structure of the influenza virus haemagglutinin complexed with its receptor, sialic acid. *Nature* **333**:426-431[Medline].
 21. Wright, C. S. 1984. Structural comparison of the two distinct sugar binding sites in wheat germ agglutination isolectin II. *J. Mol. Biol.* **178**:91-104[Medline].

Antimicrobial Agents and Chemotherapy, September 2000, p. 2578-2580, Vol. 44, No. 9
0066-4804/00/\$04.00+0

Copyright © 2000, American Society for Microbiology. All rights reserved.

- ▶ [Abstract of this Article](#)
 - ▶ [Reprint \(PDF\) Version of this Article](#)
 - ▶ Similar articles found in:
[AAC Online](#)
[PubMed](#)
 - ▶ [PubMed Citation](#)
 - ▶ Search Medline for articles by:
[Cowan, M. M.](#) || [Doyle, R. J.](#)
 - ▶ Alert me when:
[new articles cite this article](#)
 - ▶ [Download to Citation Manager](#)
- ▶ [Books from ASM Press](#)

HOME HELP FEEDBACK SUBSCRIPTIONS ARCHIVE SEARCH

Clin. Diagn. Lab. Immunol.

Clin. Microbiol. Rev.

J. Clin. Microbiol.

ALL ASM JOURNALS



**FREE Webcast of the
Keynote Presentations**

**Are you being paid
what you are *worth*?**

SCIENCE ONLINE SCIENCE MAGAZINE HOME SCIENCE NOW NEXT WAVE STKE/AIDS/SAGE SCIENCE CAREERS E-MARKETPLACE

Institution: US Patent & Trademark [fc](#) | [Sign In as Individual](#) | [FAQ](#)

Science magazine

[HELP](#) [SUBSCRIPTIONS](#) [FEEDBACK](#) [SIGN IN](#) 

[SEARCH](#)

[BROWSE](#)

[ORDER THIS ARTICLE](#)

X-ray Structure of the FimC-FimH Chaperone-Adhesin Complex from Uropathogenic *Escherichia coli*

Devapriya Choudhury,¹ Andrew Thompson,² Vivian Stojanoff,³
Solomon Langermann,⁴ Jerome Pinkner,⁵ Scott J. Hultgren,^{5*}
Stefan D. Knight^{1*}

Type 1 pili--adhesive fibers expressed in most members of the Enterobacteriaceae family--mediate binding to mannose receptors on host cells through the FimH adhesin. Pilus biogenesis proceeds by way of the chaperone/usher pathway. The x-ray structure of the FimC-FimH chaperone-adhesin complex from uropathogenic *Escherichia coli* at 2.5 angstrom resolution reveals the basis for carbohydrate recognition and for pilus assembly. The carboxyl-terminal pilin domain of FimH has an immunoglobulin-like fold, except that the seventh strand is missing, leaving part of the hydrophobic core exposed. A donor strand complementation mechanism in which the chaperone donates a strand to complete the pilin domain explains the basis for both chaperone function and pilus biogenesis.

- ▶ [Abstract of this Article](#)
- ▶ [PDF Version of this Article](#)

▶ [Download to Citation Manager](#)

▶ Alert me when:
[new articles cite this article](#)

▶ Search for similar articles in:
[Science Online](#)
[ISI Web of Science](#)
[PubMed](#)

▶ Search Medline for articles by:
[Choudhury, D.](#) || [Knight, S. D.](#)

▶ Search for citing articles in:
[ISI Web of Science \(79\)](#)
[HighWire Press Journals](#)

▶ This article appears in the following Subject Collections:
Biochemistry

¹ Department of Molecular Biology, Uppsala Biomedical Center, Swedish University of Agricultural Sciences, Box 590, S-753 24 Uppsala, Sweden.

² European Molecular Biology Laboratory Grenoble Outstation, c/o Avenue des Martyrs, BP 156X, 38042 Grenoble, France.

³ European Synchrotron Radiation Facility, Avenue des Martyrs, 38400 Grenoble, France.

⁴ MedImmune, Gaithersburg, MD 20878, USA.

⁵ Department of Molecular Microbiology, Washington University School of Medicine, St Louis, MO 63110, USA.

* To whom correspondence should be addressed. E-mail: hultgren@borcim.wustl.edu (S.J.H.); stefan@xray.bmc.uu.se (S.D.K.).

Type 1 pili are adhesive fibers expressed in *E. coli* as well as in most members of the Enterobacteriaceae family (1). They are composite structures in which a short-tip fibrillar structure containing FimG and the FimH adhesin (and possibly the minor component FimF as well) are joined to a rod composed predominantly of FimA subunits (1). The FimH adhesin mediates binding to mannose oligosaccharides (2, 3). In uropathogenic *E. coli*, this binding event has been shown to play a critical role in bladder colonization and

disease (4). Type 1 pilus biogenesis proceeds by way of a highly conserved chaperone/usher pathway that is involved in the assembly of over 25 adhesive organelles in Gram-negative bacteria (5). The usher forms an oligomeric channel in the outer membrane with a pore size of ~ 2.5 nm (6) and mediates subunit translocation across the outer membrane. Periplasmic chaperones consist of two immunoglobulin-like domains with a deep cleft between the two domains (7-9). Chaperones stabilize pilus subunits and prevent them from participating in premature interactions in the periplasm by forming chaperone-subunit complexes (5). Here, the x-ray crystal structure of the FimC-FimH chaperone-adhesin complex from uropathogenic *E. coli* is described. The structure reveals a donor strand complementation mechanism that explains the basis of both chaperone function and pilus biogenesis.

The structure of the FimC-FimH complex was solved by means of multiwavelength anomalous dispersion (MAD) data to 2.7 Å collected from selenomethionyl FimC-FimH crystals, and subsequently refined to 2.5 Å (Table 1). Eight copies of the FimC-FimH heterodimer in the C2 asymmetric unit were arranged as two sets of four molecules related by approximate 4_1 screw axes. Electron density was excellent for one set of molecules (Fig. 1A), allowing us to trace the entire complex. For the second set of molecules, electron density was poorer but allowed for unambiguous placement of a copy of the initially traced complex.

Table 1. Summary of data collection and MAD structure determination. Two seleno-methionated FimC-FimH crystals (space group C2, $a = 139.1$ Å, $b = 139.1$ Å, $c = 214.5$ Å, $\beta = 90.0^\circ$) exhibiting strong pseudo $P4_12_12$ symmetry were used to collect MAD (22) data on BM14 of the European Synchrotron Radiation Facility. Data were recorded at each of three wavelengths corresponding to the peak of the Se white line, the point of inflexion of the K absorption edge, and a remote wavelength by using a MAR charge-coupled device detector. Data were reduced with the program HKL2000 (23), with further processing and scaling using the CCP4 processing package (23). An initial solution to the Patterson function was produced in the tetragonal pseudo space group both automatically with the program SOLVE (23) and manually with the program RSPS (23), and initial phases were calculated with SHARP (23). Density modification including fourfold noncrystallographic (NCS) averaging was done with the program DM (23). A model corresponding to the two copies of the complex in the pseudo asymmetric unit was built with the program O (23). Bulk solvent correction, positional, simulated annealing, and isotropic temperature factor refinement was carried out with X-PLOR (23) and REFMAC (23) with tight NCS restraints against a 2.5 Å native data set collected at Max II/BL711 in Lund. The current R factor and R_{free} (on 5% of the data) are 24.0 and 26.8%, respectively. The root mean square deviations from ideal bond lengths and angles are 0.016 and 3.3 Å, respectively. No residues are in disallowed regions of the Ramachandran plot.

Data collection statistics							
Crystal	d_{min} (Å)	N_{unique}	Complt* (%)	Mult†	$I/\sigma(I)$ ‡	R_{sym}^{\S} (%)	$R_{\text{anom}}^{\parallel}$ (%)
SeMet Crystal 1	2.8		82.8				
Remote		93,019		2.5	13.1 (3.7)	4.0 (17.3)	3.5 (16.8)
Point of inflection		75,467		2.1	11.6 (6.9)	3.5 (24.4)	4.3 (21.4)
Peak		82,754		2.7	11.3 (1.9)	4.1 (24.7)	4.2 (18.8)
SeMet Crystal 2	2.7		98.7				

Remote	110,928	3.8	8.9 (2.0)	5.1 (28.3)	4.2 (20.9)		
Point of inflexion	110,415	4.0	10.6 (2.7)	4.2 (21.8)	3.8 (17.4)		
Peak	110,418	3.9	14.4 (2.8)	4.2 (20.8)	4.2 (17.5)		
Native	2.5 139,645 98.0	4.1	5.3 (1.6)	7.6 (25.3)	NA		
<i>Phasing statistics from SHARP</i>							
	Point of inflexion $\lambda = 0.9793 \text{ \AA}$		Peak $\lambda = 0.9792 \text{ \AA}$		Remote $\lambda = 0.885 \text{ \AA}$		
	Centric	Acentric	Centric	Acentric	Centric	Acentric	
Phasing power [¶]	2.0/—	2.1/1.2	2.0/—	2.0/1.6	—/—	—/0.81	
$R_{\text{cullis}}^{\#}$	0.49/—	0.56/0.52	0.53/—	0.54/0.57	—/—	—/0.69	
Resolution (\AA)	7.59	5.50	4.52	3.93	3.53	3.23	2.99 2.80
FOM ^{**}	0.623	0.508	0.379	0.227	0.172	0.140	0.105 0.125

* Completeness.

† Multiplicity.

‡ Overall value and values in parentheses are for the highest resolution shell.

§ $R_{\text{sym}} = \sum_h \sum_i |I_i(h) - \langle I(h) \rangle| / \sum_h \sum_i I_i(h)$, where $I_i(h)$ and $\langle I(h) \rangle$ are the intensities of the individual and mean structure factors, respectively. The high-resolution shell is in parentheses.

|| $R_{\text{anom}} = \sum_h \sum_i |I_i(h) - \langle I(h) \rangle| / \sum_h \sum_i I_i(h)$; $I_i(h)$ and $\langle I(h) \rangle$ are as defined above, and the summation is over anomalous pairs. The high-resolution shell is in parentheses.

¶ $F_H(\text{calc})/E$, where E is the estimated lack-of-closure error (isomorphous/anomalous).

$R_{\text{cullis}} = \sum ||F_{\text{PH}} - F_{\text{P}}| - F_H(\text{calc})| / \sum |F_{\text{PH}} - F_{\text{P}}|$, where F_{P} and F_{PH} are protein and heavy-atom structure factors, respectively, and $F_H(\text{calc})$ is the calculated heavy-atom structure factor (isomorphous/anomalous).

** Figure of merit for SHARP phases.



Fig. 1. (A) A typical sample of the solvent-flattened experimental electron density map (contoured at 1.0σ) with the refined model superimposed.

Arg^{8C} and Lys^{112C} anchor the COOH-terminus of FimH (Gln^{279H}) in the subunit binding cleft of the chaperone through hydrogen bonds to the terminal carboxylate. **(B)** MOLSCRIPT (24) ribbon diagram of the FimC-FimH complex. FimH is colored yellow, except for the A" (green) and F

(orange) strands of the pilin domain. FimC is colored blue, except for the G1 strand, which is cyan. The FimH pilin domain and the NH₂-terminal domain of FimC form a closed superbarrel with a continuous core made from conserved residues in both proteins. A ball-and-stick representation of the C-HEGA molecule bound to the lectin domain of FimH indicates the position of the carbohydrate-binding site at the tip of the domain. [View Larger Version of this Image (65K GIF file)]

FimH is folded into two domains of the all-beta class connected by a short extended linker (Fig. 1B). The

NH₂-terminal mannose-binding lectin domain comprises residues 1H to 156H, and the COOH-terminal pilin domain, which is used to anchor the adhesin to the pilus, comprises residues 160H to 279H (Fig. 2A). The overall structure of the FimC chaperone in the complex is essentially the same as that of the free chaperone (8, 9). The pilin domain of FimH binds in the cleft of the chaperone (Fig. 1B), although there is only limited contact between FimH and the COOH-terminal domain of FimC.

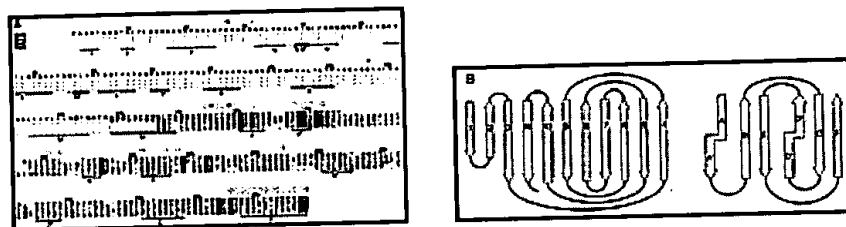


Fig. 2. (A) Alignment of type 1 pilin sequences to the pilin domain of FimH. The end of the lectin domain and the start of the pilin domain in FimH are indicated by black arrowheads above the sequences. Clustal W (25) was used to align the sequences, which were manually adjusted to minimize gaps (indicated by dots) in secondary structure elements. Residue 1 of FimH is residue 22 in the precursor protein (26). Residues are coded as follows: identical (red); conserved character (blue); pilin NH₂-terminal residues proposed to take part in donor strand complementation in the pilus (yellow); involved in chaperone binding (27) (open circle above the residue); carbohydrate binding pocket (boxed). The NH₂-terminal extensions of the pilin subunits are in one large box. Limits and nomenclature for secondary structure elements are shown below the sequence. **(B)** β -sheet topology diagrams of the lectin (left) and pilin (right) domains of FimH. Abbreviations for the amino acid residues are as follows: A, Ala; C, Cys; D, Asp; E, Glu; F, Phe; G, Gly; H, His; I, Ile; K, Lys; L, Leu; M, Met; N, Asn; P, Pro; Q, Gln; R, Arg; S, Ser; T, Thr; V, Val; W, Trp; and Y, Tyr. [View Larger Versions of these Images (34 + 18K GIF file)]

The lectin domain of FimH is an 11-stranded elongated β barrel with a jelly roll-like topology (Fig. 2B). Searches of the structural database (10, 11) did not reveal any significant structural homologs of this domain. The fold starts with a short β hairpin that is not part of the jelly roll. The final (11th) strand of the domain is inserted between the 3rd and 10th strands and thus breaks the jelly-roll topology. A pocket capable of accommodating a mono-mannose unit is located at the tip of the domain, distal from the connection to the pilin domain (Fig. 1B). A molecule of cyclohexylbutanoyl-*N*-hydroxyethyl-D-glucamide (C-HEGA) (12) is bound in this pocket (Fig. 3A). The glucamide moiety of C-HEGA is blocked at C1 and cannot form a pyranose, but is bent to approach the pyranose conformation. The C2, C3, C4, and C6 hydroxyl groups of C-HEGA are enclosed within the pocket, whereas the C5 hydroxyl and cyclohexylbutanoyl-*N*-hydroxyethyl groups point out from the pocket and are solvent exposed. Residues Asp^{54H}, Gln^{133H}, Asn^{135H}, Asp^{140H}, and the NH₂-terminal amino group of FimH (Fig. 3A) are hydrogen bonded to the glucamide moiety of C-HEGA. FimH from a urinary tract *E. coli* isolate that has a lysine instead of asparagine at position 135H produces type 1 pili but is unable to mediate mannose-sensitive hemagglutination of guinea pig erythrocytes (13). Also, a mutation at residue 136H has been reported to completely block mannose binding (14).

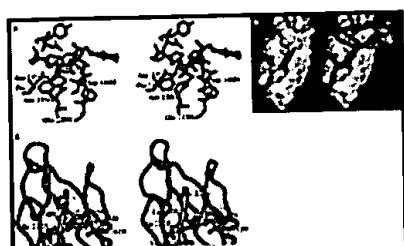


Fig. 3. (A) Stereo view of the carbohydrate binding pocket in FimH with a molecule of C-HEGA bound. Residues Phe^{1H}, Ile^{13H}, Asn^{46H}, Asp^{47H}, Tyr^{48H}, Ile^{52H}, Asp^{54H}, Gln^{133H}, Asn^{135H}, Tyr^{137H}, Asn^{138H}, Asp^{140H}, Phe^{142H} line the surface of the pocket at the tip of the lectin domain. Residues that take part in hydrogen bonding to the glucamide moiety of C-

HEGA are labeled. **(B)** (Left) Surface (28) of the FimH pilin domain showing the exposed hydrophobic core. Hydrophobic residues that are buried in the complex but solvent exposed upon removal of the chaperone are highlighted in yellow. (Right) Same as left but with FimC (blue ribbon) completing the immunoglobulin-like fold of the pilin domain. **(C)** Close-up of donor strand complementation interactions. The G1 strand of FimC (blue) donates hydrophobic residues to the core of the FimH pilin domain (yellow). The total solvent-accessible surface area that is buried between the pilin domain and the chaperone is roughly 1700 \AA^2 (on each domain). Donor strand complementation accounts for ~60% of this area.
[\[View Larger Version of this Image \(50K GIF file\)\]](#)

The pilin domain of FimH has the same immunoglobulin-like topology as the NH_2 -terminal domain of periplasmic chaperones, except that the seventh strand of the fold is missing (Fig. 2B). Two antiparallel β sheets (strands A'BED' and D''CF) pack against each other to form a β barrel that is similar to, but distinct from, immunoglobulin barrels. As in the chaperones, strand switching occurs at the edges of the sheets. In the chaperones, the A1 strand of the NH_2 -terminal domain switches between the two sheets of the barrel (15).

The first strand of the pilin domain exhibits a similar switch, but owing to the lack of a seventh strand, the second half of the A strand is not involved in main-chain hydrogen bonding within the domain. The D strand of the chaperones as well as of the FimH pilin domain also switches, but in the pilin domain the switch is an eight-residue loop instead of the cis-proline bulge found in the chaperones. The C-D loop and the D'-D'' connection pack against each other and close the top of the barrel. The other side of the barrel, defined by the A and F edge strands, is open. Owing to the absence of a seventh strand, a deep scar is created on the surface of the domain. Residues that would be part of the hydrophobic core of an intact, seven-stranded fold instead line a deep hydrophobic crevice on the surface of the pilin domain (Fig. 3B).

In the complex, the seventh (G1) strand from the NH_2 -terminal domain of the chaperone is used to complement the pilin domain by being inserted between the second half of the A strand and the F strand of the domain (Fig. 3C). The final strand (F) of FimH forms a parallel β -strand interaction with the G1 strand of FimC and has its COOH-terminal carboxylate anchored at the bottom of the chaperone cleft through hydrogen bonding with the conserved residues Arg^{8C} and Lys^{112C} in FimC (Fig. 1A). This interaction is critical for chaperone function (16, 17).

The G1 strand of periplasmic chaperones contains a conserved motif of solvent-exposed hydrophobic residues at positions 103, 105, and 107 in FimC (15). In the complex, these residues are used to complete the unfinished hydrophobic core of FimH (Fig. 3C). The two residues Leu^{103C} and Leu^{105C} are deeply buried in the crevice created in the FimH pilin domain owing to the missing seventh strand. Ile^{107C} is somewhat closer to the domain surface but makes van der Waals contacts with residues Val^{163H} and Phe^{276H}. Leu^{103C} contacts residues Ile^{181H}, Val^{223H}, Leu^{225H}, and Ile^{272H}. Leu^{105C} is in contact with Ile^{181H}, Leu^{183H}, Leu^{252H}, Ile^{272H}, and Val^{274H}. We denote this mode of binding "donor strand complementation" to emphasize the fact that the pilin domain is incomplete and that the chaperone donates its G1 strand to complete the fold. Donor strand complementation has also been observed in the recent crystal structure of the PapD-PapK complex (18).

Genetic, biochemical, and electron microscopic studies have demonstrated that residues in two conserved motifs (the COOH-terminal F strand and an NH_2 -terminal motif) participate in subunit-subunit interactions necessary for pilus assembly (17). An alignment of the pilin sequences, based on the FimC-FimH crystal

structure, revealed that the NH₂-terminal motif was part of a 10- to 20-residue NH₂-terminal extension that was missing in the FimH pilin domain (Fig. 2A) and disordered in the PapD-PapK complex (18). This region contains a pattern of alternating hydrophobic residues similar to the G1 donor strand of the chaperone. On the basis of molecular modeling, the NH₂-terminal extension of a subunit is predicted to be able to take the place of the G1 strand of the chaperone, and fit into the pilin groove. Thus, during pilus assembly, alternating hydrophobic side chains in the NH₂-terminal extension could replace the hydrophobic side chains donated to the pilin core by the G1 strand of the chaperone, through a donor strand exchange mechanism. Thus, every subunit would complete the immunoglobulin-like fold of its neighboring subunit.

The type 1 pilus is a right-handed helix with about three subunits per turn, a diameter of ~70 Å, a central pore of about 20 to 25 Å, and a pitch of about 24 Å (19). To obtain this structure, insertion of the NH₂-terminal extension must be antiparallel to strand F, in contrast to the parallel insertion observed for the G1 strand of the chaperone. Insertion in a parallel orientation would lead to rosettelike structures. Using the FimH pilin domain as a model for FimA, we constructed a model for the type 1 pilus that fit these data (Fig. 4). Each subunit was aligned to have its cleft facing toward the center of the pilus so that the height from the top to the bottom of the domain along the helix axis was ~25 Å. By applying a rotation of 115° and a rise per subunit of 8 Å, a hollow helical cylinder is created. The outer diameter of this cylinder as measured across Cα atoms is 70 Å, and the inner diameter is 25 Å. FimA subunits from different strains of *E. coli* exhibit considerable allelic variation (13). The vast majority of the variable positions are on the outside surface of the pilus model proposed above (Fig. 4), which would account for the antigenic variability of type 1 pili.

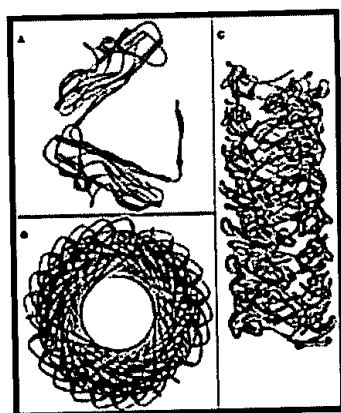


Fig. 4. Model of the type 1 pilus. The NH₂-terminal extension participates in donor strand complementation between subunits as described in the text. Subunits one turn apart in the helix pack against each other through the sides of the pilin barrel. Charged residues located between the hydrophobic side chains in the NH₂-terminal extension point into the solution on the inside of the hollow pilus rod. (A) The proposed interaction between two consecutive FimA molecules in the type 1 pilus rod. The modeled NH₂-terminal extension is colored red. (B) View of the pilus from the top. Residue positions that are subject to allelic variation (shown in blue) map to the outer surface of the pilus. (C) Side view of the pilus. [[View Larger Version of this Image \(85K GIF file\)](#)]

The proposed head-to-tail interaction between subunits in a pilus is reminiscent of oligomerization through 3D domain swapping (20), in the sense that a part of one protein molecule is used to complement another. However, in this case, complementation occurs not only between identical protein chains (FimA in the pilus rod), but also between homologous but distinct chains (for example, FimG, FimF, and FimH in the pilus tip). Furthermore, because individual pilin protomers do not exist as stable monomers, there is no exchange of structural units between a monomeric and an oligomeric state. Instead, a different protein, the periplasmic chaperone, is needed to keep the monomeric subunits in solution by donating a unique part of its structure (the G1 strand) to the different subunit grooves.

On the basis of the structure of the FimC-FimH complex, we propose that the class of proteins known as pilins are missing necessary steric information needed to fold into a native three-dimensional structure. The

information that is missing consists of the seventh-edge strand of an immunoglobulin fold. This strand, which is necessary for folding, is donated to the hydrophobic core of the pilin by the periplasmic chaperone in a donor strand complementation mechanism. A recent formulation of Anfinsen's classic postulate stated that "The steric information necessary for newly synthesized protein chains to fold correctly within cells resides solely in the primary structure of the initial translation product" (21). Here we provide an example of a case where some of that information is not inherent in the sequence of the protein to be folded but is instead transferred from another protein--the periplasmic chaperone.

REFERENCES AND NOTES

1. C. H. Jones, *et al.*, *Proc. Natl. Acad. Sci. U.S.A.* **92**, 2081 (1995) [Abstract] .
2. S. N. Abraham, D. Sun, J. B. Dale, E. H. Beachey, *Nature* **336**, 682 (1988) [ISI][Medline] .
3. K. A. Krogfelt, H. Bergmans, P. Klemm, *Infect. Immun.* **58**, 1995 (1990) [ISI][Medline] .
4. M. A. Mulvey, *et al.*, *Science* **282**, 1494 (1998) [Abstract/Full Text] .
5. G. E. Soto and S. J. Hultgren, *J. Bacteriol.* **181**, 1059 (1999) [Full Text] .
6. D. G. Thanassi, *et al.*, *Proc. Natl. Acad. Sci. U.S.A.* **95**, 3146 (1998) [Abstract/Full Text] .
7. A. Holmgren and C.-I. Brändén, *Nature* **342**, 248 (1989) [ISI][Medline] .
8. M. Pellicchia, P. Guntert, R. Glockshuber, K. Wuthrich, *Nature Struct. Biol.* **5**, 885 (1998) [CrossRef] [ISI][Medline] .
9. S. D. Knight, unpublished results.
10. G. J. Kleywegt and T. A. Jones, *Methods Enzymol.* **277**, 525 (1997) [ISI] .
11. L. Holm and C. Sander, *J. Mol. Biol.* **233**, 123 (1993) [CrossRef][ISI][Medline] .
12. C-HEGA is not a known inhibitor of FimH mannose binding but was needed in the crystallization [S. D. Knight, M. Mulvey, J. Pinkner, *Acta Crystallogr.* **D53**, 207 (1997) [ISI]] to produce useful crystals. Briefly, FimC-FimH crystals were grown by hanging drop vapor diffusion by mixing 2 μ l of a protein solution (4 mg of FimC-FimH per milliliter pre-equilibrated in 300 mM C-HEGA) with 2 μ l of reservoir solution containing 1 M ammonium sulfate in 0.1M tris-HCl buffer (pH 8.2).
13. S. Langermann, unpublished results.
14. M. A. Schembri, L. Pallesen, H. Connell, D. L. Hasty, P. Klemm, *FEMS Microbiol. Lett.* **137**, 257 (1996) [CrossRef][ISI][Medline] .
15. D. L. Hung, S. D. Knight, R. M. Woods, J. S. Pinkner, S. J. Hultgren, *EMBO J.* **15**, 3792 (1996) [Abstract] .
16. M. J. Kuehn, *et al.*, *Science* **262**, 1234 (1993) [ISI][Medline] .
17. G. E. Soto, *et al.*, *EMBO J.* **17**, 6155 (1998) [Abstract/Full Text] .
18. F. G. Sauer, G. Waksman, J. Pinkner, K. Futterer, K. W. Dodson, *Science* **285**, 1058 (1999) [Abstract/Full Text] .
19. C. C. Brinton Jr., *Trans. N.Y. Acad. Sci.* **27**, 1003 (1965) .
20. M. P. Schlunegger, M. J. Bennett, D. Eisenberg, *Adv. Protein Chem.* **50**, 61 (1997) [ISI][Medline] .
21. R. J. Ellis and F. U. Hartl, *Curr. Opin. Struct. Biol.* **9**, 102 (1999) [CrossRef][Medline] .
22. W. A. Hendrickson, *Science* **254**, 51 (1991) [ISI][Medline] .
23. Crystallographic software: HKL2000 [Z. Otwinowski and W. Minor, *Methods Enzymol.* **276**, 307 (1997) [ISI]]; CCP4 processing package [CCP4, *Acta Crystallogr.* **D50**, 760 (1994)]; SOLVE [T. C. Terwilliger and J. Berendzen, *D53*, 571 (1997)]; RSPS [S. D. Knight, I. Andersson, C.-I. Brändén, *J. Mol. Biol.* **215**, 113 (1990) [ISI][Medline]]; SHARP [E. de la Fortelle and G. Bricogne, *Methods Enzymol.* **276**, 472 (1997) [ISI]]; DM [K. D. Cowtan, *Joint CCP4 ESF-EACBM Newsl. Protein Crystallogr.* **31**, 34 (1994)]; O [T. A. Jones, J.-Y. Zou, S. W. Cowan, M. Kjeldgaard, *Acta Crystallogr.* **A47**, 110 (1991) [ISI]]; X-PLOR [A. T. Brünger, *X-PLOR Manual (Version 3.1)*: A System for X-ray Crystallography and NMR (Yale Univ. Press, New Haven, CT, 1993)]; REFMAC [G. N. Murshudov, A. A. Vagin, E. J. Dodson, *Acta Crystallogr.* **D53**, 240 (1997) [ISI]].
24. P. J. Kraulis, *J. Appl. Crystallogr.* **24**, 946 (1991) [CrossRef][ISI].
25. J. D. Thompson, D. G. Higgins, T. J. Gibson, *Nucleic Acids Res.* **22**, 4673 (1994) [Abstract] .

26. Pilus subunits are expressed in the cytoplasm as precursor proteins with an NH₂-terminal signal sequence that is cleaved during transport across the inner membrane by the Sec machinery [S. J. Hultgren, S. Normark, S. N. Abraham, *Annu. Rev. Microbiol.* **45**, 383 (1991) [ISI][Medline]]. The first visible FimH residue in our maps corresponds to Phe²² in the gene-derived sequence, which is the expected start of the mature FimH chain [M. S. Hanson, J. Hempel, C. B. Brinton Jr., *J. Bacteriol.* **170**, 3350 (1988) [ISI][Medline]]. To distinguish residues in the adhesin from residues in the chaperone, FimH residues will be denoted by an H, and FimC residues by a C, after the residue number.
27. Interface residues were defined as having a difference in solvent accessibility [S. Miller, J. Janin, A. M. Lesk, C. Chothia, *J. Mol. Biol.* **196**, 641 (1987) [ISI][Medline]] between the subunit in the complex and removed from the complex exceeding 10 percentage points.
28. A. Nicholls, *GRASP: Graphical Representation and Analysis of Surface Properties* (Columbia Univ. Press, New York, 1993).
29. We thank A. Revel and J. Burlein for technical assistance and advice; the staff at the Max II synchrotron in Lund; H. Eklund, J. Hajdu, A. Jones, and S. Ramaswamy for discussions and reading of the manuscript; and J. Berglund for help with the figures. Supported by grants from the Swedish Research Council NFR and the Swedish Foundation for Strategic Research (Structural Biology Network) (S.D.K.), and by National Institutes of Health grants RO1DK51406 and RO1AI29549 (S.J.H.). The coordinates have been deposited at the Research Collaboratory for Structural Bioinformatics Protein Data Bank (code 1QUN).

25 March 1999; accepted 14 July 1999

► [Abstract of this Article](#)

► [PDF Version of this Article](#)

► [Download to Citation Manager](#)

► Alert me when:
[new articles cite this article](#)

► Search for similar articles
in:

[Science Online](#)
[ISI Web of Science](#)
[PubMed](#)

► Search Medline for articles
by:
[Choudhury, D.](#) || [Knight, S. D.](#)

► Search for citing articles
in:
[ISI Web of Science \(79\)](#)
[HighWire Press Journals](#)

► This article appears in the
following Subject
Collections:
[Biochemistry](#)

This article has been cited by other articles:

- Thanassi, D. G., Stathopoulos, C., Dodson, K., Geiger, D., Hultgren, S. J. (2002). Bacterial Outer Membrane Ushers Contain Distinct Targeting and Assembly Domains for Pilus Biogenesis. *J. Bacteriol.* 184: 6260-6269 [[Abstract](#)] [[Full Text](#)]
- Jones, C. H., Dexter, P., Evans, A. K., Liu, C., Hultgren, S. J., Hruby, D. E. (2002). Escherichia coli DegP Protease Cleaves between Paired Hydrophobic Residues in a Natural Substrate: the PapA Pilin. *J. Bacteriol.* 184: 5762-5771 [[Abstract](#)] [[Full Text](#)]
- Mu, X.-Q., Egelman, E. H., Bullitt, E. (2002). Structure and Function of Hib Pili from Haemophilus influenzae Type b. *J. Bacteriol.* 184: 4868-4874 [[Abstract](#)] [[Full Text](#)]
- Kjaergaard, K., Hasman, H., Schembri, M. A., Klemm, P. (2002). Antigen 43-Mediated Autotransporter Display, a Versatile Bacterial Cell Surface Presentation System. *J. Bacteriol.* 184: 4197-4204 [[Abstract](#)] [[Full Text](#)]
- Bann, J. G., Pinkner, J., Hultgren, S. J., Frieden, C. (2002). Real-time and equilibrium 19F-NMR studies reveal the role of domain-domain interactions in the folding of the chaperone PapD. *Proc. Natl. Acad. Sci. U. S. A.* 99: 709-714 [[Abstract](#)] [[Full Text](#)]
- Zhou, G., Mo, W.-J., Sebbel, P., Min, G., Neubert, T. A., Glockshuber, R., Wu, X.-R., Sun, T.-T., Kong, X.-P. (2002). Uroplakin Ia is the urothelial receptor for uropathogenic Escherichia coli: evidence from in vitro FimH binding. *J. Cell Sci* 114: 4095-4103 [[Abstract](#)] [[Full Text](#)]
- Choi, B.-K., Schifferli, D. M. (2001). Characterization of FasG Segments Required for 987P Fimbria-Mediated Binding to Piglet Glycoprotein Receptors. *Infect. Immun.* 69: 6625-6632 [[Abstract](#)] [[Full Text](#)]
- Edwards, R. A., Matlock, B. C., Heffernan, B. J., Maloy, S. R. (2001). Genomic analysis and growth-phase-dependent regulation of the SEF14 fimbriae of Salmonella enterica serovar Enteritidis. *Microbiology* 147: 2705-2715 [[Abstract](#)] [[Full Text](#)]
- Lee, V. T., Schneewind, O. (2001). Protein secretion and the pathogenesis of bacterial infections. *Genes & Dev.* 15: 1725-1752 [[Full Text](#)]
- Cobbald, C., Windsor, M., Wileman, T. (2001). A Virally Encoded Chaperone Specialized for Folding of the Major Capsid Protein of African Swine Fever Virus. *J. Virol.* 75: 7221-7229 [[Abstract](#)] [[Full Text](#)]
- Sung, M.-a., Fleming, K., Chen, H. A., Matthews, S. (2001). The solution structure of PapGII from uropathogenic Escherichia coli and its recognition of glycolipid receptors. *EMBO Reports* 2: 621-627 [[Abstract](#)] [[Full Text](#)]
- Schembri, M. A., Klemm, P. (2001). Coordinate gene regulation by fimbriae-induced signal transduction. *EMBO J.* 20: 3074-3081 [[Abstract](#)] [[Full Text](#)]
- Harris, S. L., Spears, P. A., Havell, E. A., Hamrick, T. S., Horton, J. R., Orndorff, P. E. (2001). Characterization of Escherichia coli Type 1 Pilus Mutants with Altered Binding Specificities. *J. Bacteriol.* 183: 4099-4102 [[Abstract](#)] [[Full Text](#)]
- Hooper, L. V., Gordon, J. I. (2001). Glycans as legislators of host-microbial interactions: spanning the spectrum from symbiosis to pathogenicity. *Glycobiology* 11: 1R-10 [[Abstract](#)] [[Full Text](#)]
- Hung, D. L., Raivio, T. L., Jones, C.H., Silhavy, T. J., Hultgren, S. J. (2001). Cpx signaling pathway monitors biogenesis and affects assembly and expression of P pili. *EMBO J.* 20: 1508-1518 [[Abstract](#)] [[Full Text](#)]
- Zavialov, A. V., Batchikova, N. V., Korpela, T., Petrovskaya, L. E., Korobko, V. G., Kersley, J., MacIntyre, S., Zav'yalov, V. P. (2001). Secretion of Recombinant Proteins via the Chaperone/Usher Pathway in Escherichia coli. *Appl. Environ. Microbiol.* 67: 1805-1814 [[Abstract](#)] [[Full Text](#)]
- Harrison, P. M., Chan, H. S., Prusiner, S. B., Cohen, F. E. (2001). Conformational propagation with prion-like characteristics in a simple model of protein folding. *Protein Sci* 10: 819-835 [[Abstract](#)] [[Full Text](#)]
- Schembri, M. A., Klemm, P. (2001). Biofilm Formation in a Hydrodynamic Environment by Novel FimH Variants and Ramifications for Virulence. *Infect. Immun.* 69: 1322-1328 [[Abstract](#)] [[Full Text](#)]
- Augustine, J. G., de la Calle, A., Knarr, G., Buchner, J., Frederick, C. A. (2001). The Crystal Structure

of the Fab Fragment of the Monoclonal Antibody MAK33. IMPLICATIONS FOR FOLDING AND INTERACTION WITH THE CHAPERONE BiP. *J. Biol. Chem.* 276: 3287-3294

- Schilling, J. D., Mulvey, M. A., Vincent, C. D., Lorenz, R. G., Hultgren, S. J. (2001). Bacterial Invasion Augments Epithelial Cytokine Responses to Escherichia coli Through a Lipopolysaccharide-Dependent Mechanism. *The JI* 166: 1148-1155 [[Abstract](#)] [[Full Text](#)]
- Tanskanen, J., Saarela, S., Tankka, S., Kalkkinen, N., Rhen, M., Korhonen, T. K., Westerlund-Wikström, B. (2001). The gaf Fimbrial Gene Cluster of Escherichia coli Expresses a Full-Size and a Truncated Soluble Adhesin Protein. *J. Bacteriol.* 183: 512-519 [[Abstract](#)] [[Full Text](#)]
- Klemm, P., Schembri, M. A. (2000). Fimbrial surface display systems in bacteria: from vaccines to random libraries. *Microbiology* 146: 3025-3032 [[Full Text](#)]
- Hamrick, T. S., Harris, S. L., Spears, P. A., Havell, E. A., Horton, J. R., Russell, P. W., Orndorff, P. E. (2000). Genetic Characterization of Escherichia coli Type 1 Pilus Adhesin Mutants and Identification of a Novel Binding Phenotype. *J. Bacteriol.* 182: 4012-4021 [[Abstract](#)] [[Full Text](#)]
- Karlsson, K.-A. (2000). The human gastric colonizer Helicobacter pylori: a challenge for host-parasite glycobiology. *Glycobiology* 10: 761-771 [[Abstract](#)] [[Full Text](#)]
- Mulvey, M. A., Schilling, J. D., Martinez, J. J., Hultgren, S. J. (2000). From the Cover: Bad bugs and beleaguered bladders: Interplay between uropathogenic Escherichia coli and innate host defenses. *Proc. Natl. Acad. Sci. U. S. A.* 97: 8829-8835 [[Abstract](#)] [[Full Text](#)]
- Saulino, E. T., Bullitt, E., Hultgren, S. J. (2000). Snapshots of usher-mediated protein secretion and ordered pilus assembly. *Proc. Natl. Acad. Sci. U. S. A.* 97: 9240-9245 [[Abstract](#)] [[Full Text](#)]
- Weaver, A. J., Sullivan, W. P., Felts, S. J., Owen, B. A. L., Toft, D. O. (2000). Crystal Structure and Activity of Human p23, a Heat Shock Protein 90 Co-chaperone. *J. Biol. Chem.* 275: 23045-23052 [[Abstract](#)] [[Full Text](#)]
- Normark, S. (2000). Anfinsen comes out of the cage during assembly of the bacterial pilus. *Proc. Natl. Acad. Sci. U. S. A.* 97: 7670-7672 [[Full Text](#)]
- Barnhart, M. M., Pinkner, J. S., Soto, G. E., Sauer, F. G., Langermann, S., Waksman, G., Frieden, C., Hultgren, S. J. (2000). From the Cover: PapD-like chaperones provide the missing information for folding of pilin proteins. *Proc. Natl. Acad. Sci. U. S. A.* 97: 7709-7714 [[Abstract](#)] [[Full Text](#)]
- Martinez, J. J., Mulvey, M. A., Schilling, J. D., Pinkner, J. S., Hultgren, S. J. (2000). Type 1 pilus-mediated bacterial invasion of bladder epithelial cells. *EMBO J.* 19: 2803-2812 [[Abstract](#)] [[Full Text](#)]
- Schembri, M. A., Sokurenko, E. V., Klemm, P. (2000). Functional Flexibility of the FimH Adhesin: Insights from a Random Mutant Library. *Infect. Immun.* 68: 2638-2646 [[Abstract](#)] [[Full Text](#)]
- Edwards, R. A., Schifferli, D. M., Maloy, S. R. (2000). A role for Salmonella fimbriae in intraperitoneal infections. *Proc. Natl. Acad. Sci. U. S. A.* 97: 1258-1262 [[Abstract](#)] [[Full Text](#)]
- Sauer, F. G., Fütterer, K., Pinkner, J. S., Dodson, K. W., Hultgren, S. J., Waksman, G. (1999). Structural Basis of Chaperone Function and Pilus Biogenesis. *Science* 285: 1058-1061 [[Abstract](#)] [[Full Text](#)]

Volume 285, Number 5430, Issue of 13 Aug 1999, pp. 1061-1066.

Copyright © 1999 by The American Association for the Advancement of Science. All rights reserved.

Are you being paid
what you are worth?